

Power transmission system midpoint voltage fixation using SVC with genetic tuned simple PID controller

Mohanad Azeez Joodi ¹, Ibraheem Kasim Ibraheem ^{1*}, Firas Mohammed Tuaimah ¹

¹ Electrical Engineering Department College of Engineering University of Baghdad Baghdad, Iraq

*Corresponding author E-mail: ibraheem.i.k@iee.org

Abstract

Contingency in power system is widely used to predict the effect of outages in power systems, like failures of equipment, transmission line, etc. The transmission system voltage will be affected due to these contingencies. To stabilize its voltage, especially the midpoint voltage, the Static VAR Compensator (SVC) is one of the shunt connected devices, which can be utilized for voltage fixation in power systems. The dynamic equations for the Single-Machine-Infinite-Bus (SMIB) SVC model will be presented which is expressed in terms of linearized state-space equations. Then, with the aid of MATLAB, the plant of the system model will be given under various loading conditions, and four suggested scenarios have been proposed as contingencies in the power transmission system. The SVC will be controlled using a simple PID controller tuned through the Genetic algorithm, the results were promising, and the midpoint voltage step response has been enhanced.

Keywords: Contingency; SVC; PID Controller; Genetic Algorithm; Power Transmission; SMIB.

1. Introduction

In power systems, maintaining voltage stability is a crucial mission to power engineers. To achieve this mission, Flexible AC Transmission Systems (FACTS) are used. One of the FACT systems that are widely used nowadays is the Static VAR compensator (SVC), where usually it is placed at the midpoint of the power transmission lines, and its output is varied via a controller to exchange capacitive or inductive current to regain the original operating condition [1]. The optimum location of the SVC has been examined in [2, 3]. The SVCs utilize power electronic devices to improve existing power network parameters; typically, the bus voltage [4]. They can be of significant advantage due to its capabilities of stabilizing bus voltage, reducing power transmission losses, increasing power transmission capacity, deferring the need for installation of new transmission lines and many other [1].

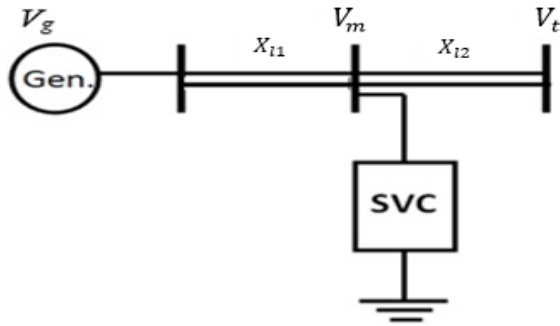
Recently, the aforementioned SVCs advantages of the are investigated by many researchers, wherein [5] authors designed a robust damping controller for Single machine Infinite Bus bar (SMIB) system with SVC installed at the middle of the power transmission lines. A robust damping controller has been designed through Static Compensator (STATCOM) devices using H-infinity loop shaping technique [6]. Involving the Artificial Neural Networks (ANN) in the design of the SVC are discussed in [7]–[9], where [7] proposed a novel idea of applying ANN based SVC controller for voltage stability improvement in an isolated wind-diesel hydro hybrid system. A PID controller tuned with ANN has been developed in [8] to improve the response of the SVC. While an SVC controller is based on the discrete-time filtered direct control theory by which a multilayer ANN is derived in [9]. On the other hand, fuzzy logic based supplementary controller for SVC is developed in [10]–[14]. A PI-based SVC controller is added to a SMIB system [15], where different effects of this controller such as rapidity and stability are presented and discussed. It is worthy of mentioning that that SVC

system can be integrated with any other types of controllers, like, H-infinity [16]–[18], LQG [19], Fractional control [20], and possibly a PID controller with swarm based optimization tuning algorithm [21]. The shortcomings of the above studies are due to a long time the adaptation process this controller takes as the case of NN based controllers or the complexities of the implementation such as the case of fuzzy logic or H-infinity based SVC supplementary controllers. In this paper, a genetic tuned simple PID controller is proposed and applied to the SMIB system with an SVC installed in the middle of the power transmission lines. The purpose of the PID controller is to maintain the voltage stability of the midpoint of the power transmission line in case of sudden load change and power transmission reconfiguration due to faults or switching. Moreover, the simulations for SMIB are presented and discussed.

2. Problem statement and SVC modeling

In this paper, an SVC (Static Var Compensator) will be connected on a Single Machine Infinite Bus System (SMIB) which consists of a synchronous generator and double transmission line as shown in Fig. 1. The system dynamics is described by the following equations [5],

$$\begin{cases} \dot{\delta} = \omega - \omega_0 \\ \dot{\omega} = \frac{\omega_0}{2H} (P_m - P_e) - \frac{D}{2H} (\omega - \omega_0) \\ \dot{B}_L = \frac{K}{T} [-B_L + B_{Lo} + K_c u] \end{cases} \quad (1)$$


Fig. 1: Single Machine Infinite Bus System with SVC.

Where

$$P_e = \frac{V_g V_t}{X_{l1} + X_{l2} + X_{l1} X_{l2} (B_L - B_C)} \sin \delta \quad (2)$$

The parameters in the equations above are shown in Table 1, while the values of these parameters are listed in the appendix.

Table 1: System parameters and definitions

Symbol	Definition
δ	Power angle of the generator in radian
ω_o	Relative speed in radian
ω	Relative speed in radian
P_m	Mechanical input power (in p.u.)
P_e	Electric input power in the generator (in p.u.)
D	Damping constant (in p.u.)
H	Inertia constant of the generator (in sec.)
X_{l1}, X_{l2}	Reactances (in p.u.)
V_g	Transient EMF of generator (in p.u.)
V_t	Infinite bus voltage(in p.u.)
B_C	Susceptance of the equivalent capacitor (in p.u.)
B_L	Susceptance of the inductor in SVC (in p.u.)
B_{Lo}	The initial value of the BL (in p.u.)
K	Control gain of SVC(in p.u.)
T	The time constant of SVC
K_C	The gain in the control loop (in p.u.)

The mid-bus voltage V_m can be written as,

$$V_m = \sqrt{\frac{(X_{l2} V_g \cos \delta + X_{l1} V_t)^2 + (X_{l2} V_g \sin \delta)^2}{X_{l1} + X_{l2} + X_{l1} X_{l2} (B_L - B_C)}} \quad (3)$$

where V_m is the mid-bus voltage? The dynamics of the synchronous generator, based on (1) and (2), can be written in a state-space form as,

$$\begin{cases} \dot{X}(t) = f(x, u) \\ Y(x) = g(x, u) \end{cases} \quad (4)$$

where

$$x = [\delta \quad \omega \quad B_L]^T \quad (5)$$

$$g(x) = [\delta \quad \omega \quad V_m]^T \quad (6)$$

$$f(x, u) = \begin{bmatrix} f_1(x, u) \\ f_2(x, u) \\ f_3(x, u) \end{bmatrix} = \begin{bmatrix} \frac{\omega - \omega_o}{2H} P_m - \frac{\omega_o}{2H} P_e - \frac{D}{2H} \omega + \frac{D}{2H} \omega_o \\ -\frac{K}{T} B_L + \frac{K}{T} B_{Lo} + \frac{K K_C}{T} u \end{bmatrix} \quad (7)$$

Linearizing the nonlinear SVC model of (1-3) around the equilibrium point, the linearized state-space matrices can be derived as follows,

$$A = \frac{df(x, u)}{dx} = \begin{bmatrix} \frac{df_1(x, u)}{dx_1} & \frac{df_1(x, u)}{dx_2} & \frac{df_1(x, u)}{dx_3} \\ \frac{df_2(x, u)}{dx_1} & \frac{df_2(x, u)}{dx_2} & \frac{df_2(x, u)}{dx_3} \\ \frac{df_3(x, u)}{dx_1} & \frac{df_3(x, u)}{dx_2} & \frac{df_3(x, u)}{dx_3} \end{bmatrix} = \begin{bmatrix} 0 & 1 & 0 \\ a_{21} & \frac{-D}{2H} & a_{23} \\ 0 & 0 & \frac{-K}{T} \end{bmatrix} \quad (8)$$

Where

$$a_{21} = \frac{-\omega_o}{2H} \frac{V_g V_t \cos \delta}{X_{l1} + X_{l2} + X_{l1} X_{l2} (B_L - B_C)}$$

$$a_{23} =$$

$$\frac{-\omega_o}{2H} \left(\frac{V_g V_t X_{l1} X_{l2} \sin \delta}{(X_{l1} + X_{l2})^2 + 2(X_{l1} + X_{l2})(X_{l1} X_{l2} (B_L - B_C)) + X_{l1}^2 X_{l2}^2 (B_L - B_C)^2} \right)$$

$$B = \frac{df(x, u)}{du} = \begin{bmatrix} \frac{df_1(x, u)}{du} \\ \frac{df_2(x, u)}{du} \\ \frac{df_3(x, u)}{du} \end{bmatrix} = \begin{bmatrix} 0 \\ 0 \\ \frac{K_1 K_C}{T} \end{bmatrix} \quad (9)$$

$$C = \frac{dg(x, u)}{dx} = \begin{bmatrix} \frac{dg_1(x, u)}{dx_1} & \frac{dg_1(x, u)}{dx_2} & \frac{dg_1(x, u)}{dx_3} \\ \frac{dg_2(x, u)}{dx_1} & \frac{dg_2(x, u)}{dx_2} & \frac{dg_2(x, u)}{dx_3} \\ \frac{dg_3(x, u)}{dx_1} & \frac{dg_3(x, u)}{dx_2} & \frac{dg_3(x, u)}{dx_3} \end{bmatrix} = \begin{bmatrix} C_1 \\ C_2 \\ C_3 \end{bmatrix} = \begin{bmatrix} 1 & 0 & 0 \\ 0 & 1 & 0 \\ c_{31} & 0 & c_{33} \end{bmatrix} \quad (10)$$

where

$$c_{31} = \frac{-2(X_{l2} V_g \cos \delta + X_{l1} V_t)(X_{l2} V_g \sin \delta) + (X_{l2} V_g)^2 \sin 2\delta}{2*(X_{l1} + X_{l2} + X_{l1} X_{l2} (B_L - B_C))} *$$

$$\frac{1}{\sqrt{(X_{l2} V_g \cos \delta + X_{l1} V_t)^2 + (X_{l2} V_g \sin \delta)^2}}$$

$$c_{33} = -\frac{X_{l1} X_{l2} \sqrt{(X_{l2} V_g \cos \delta + X_{l1} V_t)^2 + (X_{l2} V_g \sin \delta)^2}}{[X_{l1} + X_{l2} + X_{l1} X_{l2} (B_L - B_C)]^2}$$

$$D = \frac{dg(x, u)}{du} = \begin{bmatrix} \frac{dg_1(x, u)}{du} \\ \frac{dg_2(x, u)}{du} \\ \frac{dg_3(x, u)}{du} \end{bmatrix} = \begin{bmatrix} 0 \\ 0 \\ 0 \end{bmatrix} \quad (11)$$

2.1. System transfer functions for different loading conditions

The electric power P_e produced by the generator given in (2) for natural loading condition, i.e., $P_e = P_o = 0.4$ will be calculated as given below. Substituting the sample data for power system parameters given in the appendix in (2), a relationship between the power angle δ and the susceptance B_L of the inductor in the SVC

$$0.4 = P_e = \frac{1.1 * 1}{0.45 + 0.3 + 0.45 * 0.3 (B_L - 0.8)} \sin \delta$$

$$\sin \delta = 0.23345 + 0.049 B_L \quad (12)$$

It is required to maintain $V_m = 1$ p.u in (3) under different loading conditions, i.e.,

$$1 = \frac{\sqrt{(0.3*1.1*\cos\delta+0.45*1)^2+(0.3*1.1*\sin\delta)^2}}{0.45+0.3+0.45*0.3(B_L-0.8)}$$

After several steps of simplifications, the following equation will be observed,

$$\cos \delta = 0.05824B_L + 0.06B_L^2 + 0.3387 \quad (13)$$

Since, $\cos^2 \delta + \sin^2 \delta = 1$

$$\therefore \cos \delta = \sqrt{1 - \sin^2 \delta} \quad (14)$$

By substituting (14) in (13),

$$\sqrt{1 - \sin^2 \delta} = 0.05824B_L + 0.06B_L^2 + 0.3387 \quad (15)$$

Solving (15) and (12) for B_L and δ , the results is,

$$0.05824B_L + 0.06B_L^2 + 0.3387 = \sqrt{1 - (0.23345 + 0.049B_L)^2}$$

By squaring the two sides and after several steps of simplifications, the following will be observed

$$0.0036B_L^4 + 0.0698B_L^3 + 0.382041B_L^2 + 0.41688B_L - 0.8308 = 0$$

The roots of this equation are: -10.6056, -6.0386, -3.7147 and 0.9701. By neglecting the negative values, $B_L = 0.9701$. Substitute in eq. (1)

$$\sin \delta = 0.23345 + 0.049*0.9701, \therefore \delta = 0.285 \text{ rad} = 16.32^\circ$$

To obtain the open-loop transfer function of the SMIB-SVC system, substitute the power system data and the values of B_L and δ in state-space equations (8), (9), (10) and (11). The MATLAB command `ss2tf` has been used to convert A , B , C , and D state-space matrices to transfer function,

$$TF = \frac{y}{u} = \frac{V_m}{u} = \frac{27.78s^2 + 0.4584s + 43860}{s^3 + 6.016s^2 + 1545s + 9268} \quad (16)$$

Where $y = V_m = C_1x + Du$. The same procedure can be followed in order to obtain the transfer function at the other loading conditions.

At $P_o=0.6$, the transfer function will be:

$$TF = \frac{V_m}{u} = \frac{27.44s^2 + 0.4528s + 42940}{s^3 + 6.016s^2 + 1482s + 8891} \quad (17)$$

At $P_o=0.8$,

$$TF = \frac{V_m}{u} = \frac{26.95s^2 + 0.4447s + 41880}{s^3 + 6.016s^2 + 1393s + 8356} \quad (18)$$

At $P_o=1$,

$$TF = \frac{V_m}{u} = \frac{26.28s^2 + 0.4336s + 40870}{s^3 + 6.016s^2 + 1273s + 7635} \quad (19)$$

At $P_o=1.2$,

$$TF = \frac{V_m}{u} = \frac{25.4s^2 + 0.419s + 40240}{s^3 + 6.016s^2 + 1118s + 6705} \quad (20)$$

These transfer functions will be used in the closed-loop simulations shown in Fig. 2. In our simulations, the cost function $f(t)$ to be minimized is taken as the Integral Time Absolute Error (ITAE) defined as,

$$f(t) = ITAE = \int_0^\infty t|e(t)|dt \quad (21)$$

where t is the simulation time and $e(t)$ is the difference between the set point V_m voltage and the controlled V_m . It is more common to state the objective of GA as the maximization of some utility or fitness function given by,

$$F(t) = \frac{1}{1+f(t)} \quad (22)$$

where $f(t)$ is the cost function to be minimized?

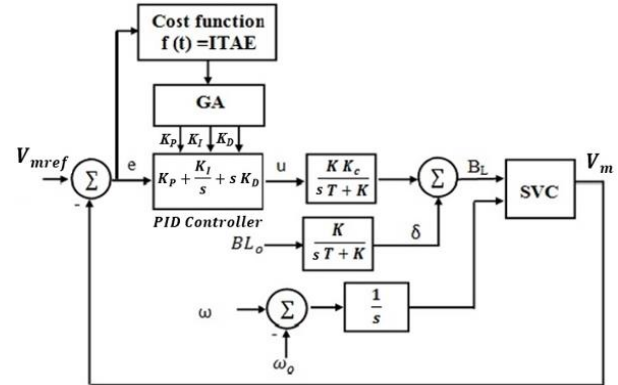


Fig. 2: Closed-Loop SVC Using Genetic-Based PID Controller.

3. Proposed genetic-based PID controller in SVC system

This section explicitly details the processing of the proposed GA tuned PID controller for the SVC system connected with SMIB.

3.1. SVC control system based on genetic-tuned PID controller

The detailed steps for the design of PID controller using GA are listed below:

- Initialize the system parameters of the SVC model.
- Initialize GA parameters: population size, variable bounds, fitness function, the maximum number of iterations, crossover probability (PC), mutation probability (PM), permissible.
- value of the standard deviation of the fitness values of the population (sd)max.
- Create a random population; each population is of a chromosome defined as,

K_{P1}	K_{I1}	K_{D1}	...	K_{Pm}	K_{Im}	K_{Dm}
----------	----------	----------	-----	----------	----------	----------
- Carry out the reproduction, crossover with probability PC, and mutation with probability PM.
- Perform the closed loop simulation for each chromosome (i.e., for each K_P , K_I and K_D set).
- Evaluate the fitness function F_i of the new population, where $i=1, \dots, m$.
- Test the convergence of the algorithm, If $sd \leq (sd)_{max}$, then stop. Otherwise, go to step 8.
- Test of the maximum number of generations, if yes stop, otherwise go to step 4.

3.2. Proposed contingency analysis

Contingencies are defined as potentially harmful disturbances that occur during the steady-state operation of a power system. A power system which is operating under normal mode may face contingencies such as sudden loss of line or generator, sudden increase or decrease of power demand. These contingencies cause transmission line overloading or bus voltage violations. In electrical power systems, voltage stability is receiving special attention these days. Substantial violations in transmission line flow can result in line outage which may lead to a cascading effect of outages and cause overload on the other lines. If such overload results from a

line outage there is an immediate need for the control action to be initiated for the line overload alleviation. Therefore contingency analysis is one of the most important tasks to be met by the power system planners and operation engineers. But online contingency analysis is difficult because of the conflict between the accuracy in a solution of the power system problem and the speed required to simulate all the contingencies. The simulation of contingency is complex since it results in a change in the configuration of the system. The SVC is placed at the middle of the transmission lines(two lines in parallel before and after the SVC) which is generally considered to be the ideal site. Since the location of SVC strongly affects controllability of the swing modes, so the best location is at a point where voltage swings are the greatest. Normally, the midpoint of a transmission line is a good candidate for placement.

4. Simulations results and discussion

In this section, the effectiveness of the SVC on fixing the transmission line midpoint voltage controlled via an SVC system with a GA tuned PID controller will be presented, where the simulations were built using a MATLAB simulator.

Four scenarios have been suggested to check the PID controller effectiveness in fixation of the midpoint voltage V_m , and as follows:

- a) Scenario A: different loading operating conditions ($P_e = 0.4, 0.6, 0.8, 1$ and 1.2).
- b) Scenario B: different loading operating conditions ($P_e = 0.4, 0.6, 0.8, 1$ and 1.2) and one line disconnected of X_{11} .
- c) Scenario C: different loading operating conditions ($P_e = 0.4, 0.6, 0.8, 1$ and 1.2) and one line disconnected of X_{12} .
- d) Scenario D: different loading operating conditions ($P_e = 0.4, 0.6, 0.8, 1$ and 1.2) and one line disconnected of X_{11} and one line disconnected of X_{12}

Tables (2-5) shows the simulation results of the midpoint step response (steady-state error Ess , settling time Ts , rise time Tr , and peak overshoot Mp) for all the pre-mentioned scenarios. Fig. 3 shows the output voltage response (V_m) for the open-loop system including the SVC system without control.

It can be seen from Fig. 1 that the system does not meet the specified limits of the voltage which one p.u. Figs. 4. (a-h) confirm the results of Tables (1-4) for the midpoint voltage step response with different loading conditions and contingencies (i.e., the four scenarios for two loading conditions, which is the minimum one ($P_e=0.4$) and the maximum one ($P_e=1.2$)).

As can be seen from these Figs., the midpoint bus voltage V_m remains fixed around the desired one (1 p.u) due to the effectiveness of the proposed genetic-based PID controller. The overshoot and the steady state error are within the acceptable range and the rise time was very small for almost all the loading conditions and contingencies.

Table 2: Midpoint Voltage Step Response (Scenario A)

	$P_e=0.4$	$P_e=0.6$	$P_e=0.8$	$P_e=1$	$P_e=1.2$
Ess	4.95e-06	3.02e-06	3.86e-06	9.91e-07	9.91e-07
Tr	0.85	0.74	0.63	0.68	3.15
Ts	5.45	9.54	64.23	136.86	201.35
Mp	0.010	0.018	0.021	0.023	0.026
Kp	99.90	99.99	99.94	99.28	99.88
KI	99.63	99.99	99.77	99.74	99.65
KD	58.49	86.48	99.60	99.634	99.76

Table 3: Midpoint Voltage Step Response (Scenario B)

	$P_e=0.4$	$P_e=0.6$	$P_e=0.8$	$P_e=1$	$P_e=1.2$
Ess	3.73e-06	4.09e-06	4.11e-06	4.05e-06	4.14e-06
Tr	0.85	0.65	0.60	0.60	0.60
Ts	5.51	8.31	9.14	9.53	9.32
Mp	0.0845	0.0755	0.0729	0.0732	0.072
Kp	99.90	99.99	99.94	99.28	99.88
KI	99.63	99.99	99.77	99.74	99.65
KD	58.49	86.48	99.60	99.63	99.76

Table 4: Midpoint Voltage Step Response (Scenario C)

	$P_e=0.4$	$P_e=0.6$	$P_e=0.8$	$P_e=1$	$P_e=1.2$
Ess	3.51e-06	3.03e-06	3.26e-07	2.18e-06	3.23e-06
Tr	0.81	0.60	0.56	0.58	0.57
Ts	7.93	9.32	9.74	9.72	9.32
Mp	0.078	0.069	0.0671	0.0673	0.0671
Kp	99.90	99.99	99.94	99.288	99.88
KI	99.63	99.99	99.77	99.74	99.65
KD	58.49	86.48	99.60	99.63	99.76

Table 5: Mid-Point Voltage Step Response (Scenario D)

	$P_e=0.4$	$P_e=0.6$	$P_e=0.8$	$P_e=1$	$P_e=1.2$
Ess	1.68e-06	7.86e-07	1.74e-06	5.69e-08	1.62e-06
Tr	0.74	0.54	0.511	0.523	0.509
Ts	86.55	52.45	40.87	39.40	40.13
Mp	0.060	0.054	0.0521	0.0523	0.0521
Kp	99.90	99.99	99.94	99.28	99.88
KI	99.63	99.99	99.77	99.74	99.65
KD	58.49	86.48	99.601	99.63	99.76

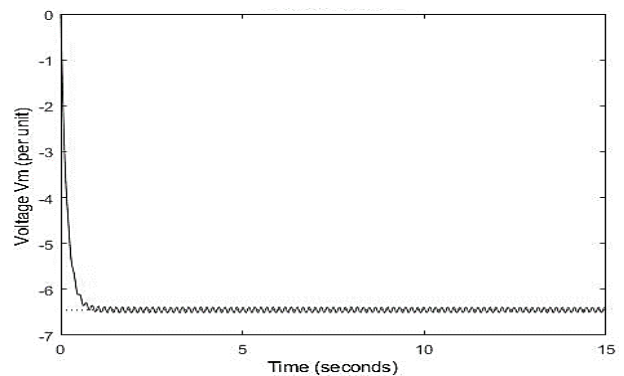
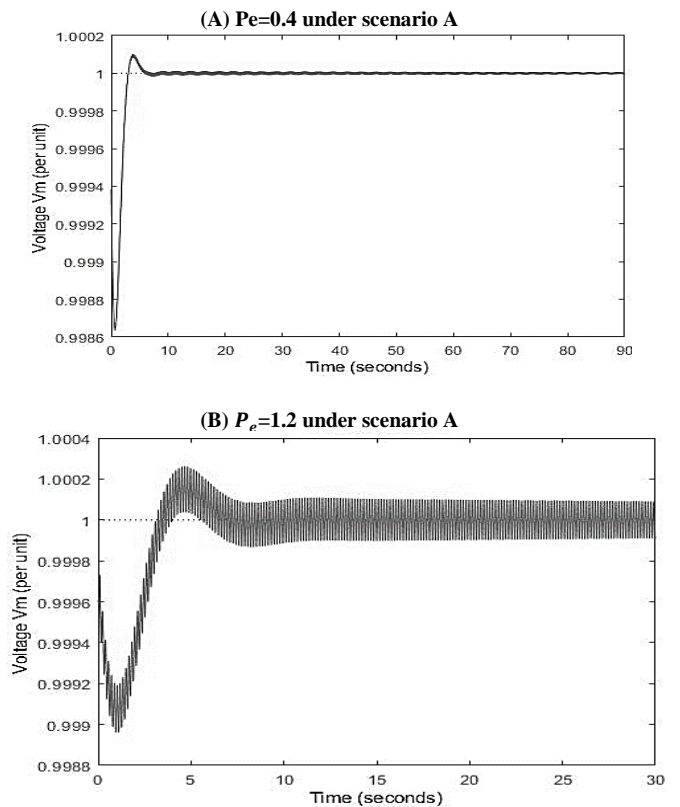


Fig. 3: The No-Control SVC Response.



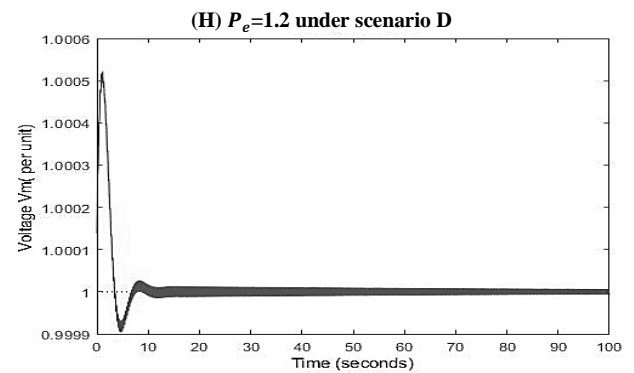
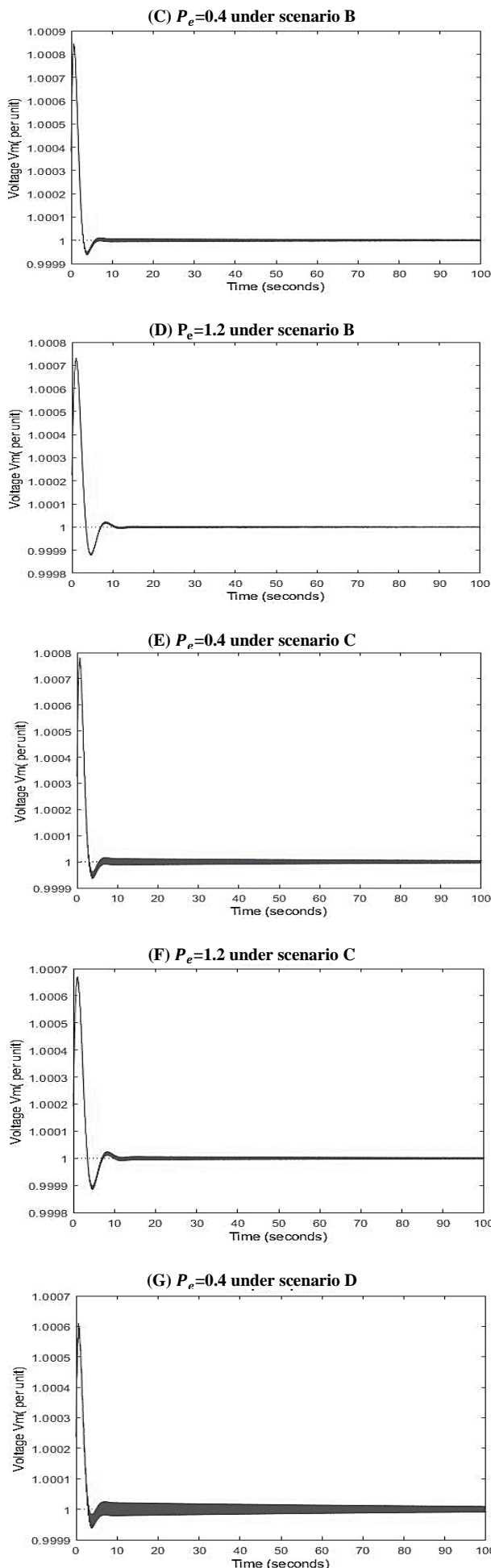


Fig. 4: Closed-Loop SVC Using Genetic-Based PID Controller.

5. Conclusion

This paper aims at power system stability enhancement via genetic-tuned PID based SVC-controller. The SVC is investigated by connecting it in a SMIB power system for voltage regulation enhancement and fixation on the transmission line. The performance evaluation of the proposed genetic-tuned PID based SVC-controller has been carried out under four suggested scenarios related to power loading and line disconnection as contingencies. Because of the insertion of the SVC, the reactance of the transmission line was changed. The electrical variables were changed also depending on the susceptance of the SVC. The results showed a useful enhancement for midpoint voltage based on the proposed system in comparison with the no-control SVC system.

References

- [1] M. Eremia, C. C. Liu, A. A. Edris, *Advanced solutions in power systems: hvdc, facts, and artificial intelligence*, IEEE Press, 2016.
- [2] F. M. Tuaimah, Y. N. Al-Aani, H. A. A. Salbi, Optimal location of static synchronous compensator (statcom) for IEEE 5-bus standard system using genetic algorithm, *Journal of Engineering*, vol. 21, no. 7, 2015, pp. 72–84.
- [3] H. A. Hassonny and F. M. Tuaimah, K. Pfeiffer, V / VAR Control for the Iraqi national SHV grid by optimum placement of svc using genetic algorithm, *International journal of Computer Applications*, vol. 66, no. 12, 2013, pp. 27–32.
- [4] K. L. Lo, L. Khan, Fuzzy logic based SVC for power system transient stability enhancement, *International Conference on Electric Utility Deregulation and Restructuring and Power Technologies*, London, UK, 2000, pp. 453–458. doi:10.1109/DRPT.2000.855707.
- [5] S. A. Al-baiyat, Design of a robust SVC damping controller using nonlinear H_∞ technique, *Arab. J. Sci. Eng.*, vol. 30, no. 1B, 2005, pp. 65–80.
- [6] A. H. M. A. Rahim, S. A. Al-Baiyat, and H. M. Al-Maghrabi, Robust damping controller design for a static compensator, *IEEE Proceedings-Generation, Transm. Distrib.*, vol. 149, no. 4, 2002, pp. 491–496.
- [7] A. Mohanty, M. Viswawandya, S. Mohanty, and D. K. Mishra, Intelligent controller based svc for voltage stability improvement in a stand-alone wind-diesel-micro hydro hybrid system, *Procedia Comput. Sci.*, vol. 57, 2015, pp. 1308–1316.
- [8] A. H. M. Afaneen A. Abood, F. M. Tuaimah, Modeling of SVC controller based on adaptive pid controller using neural networks, *Int. J. Comput. Appl.*, vol. 59, no. 6, 2012, pp. 9–16.
- [9] H. Wang and O. P. Malik, Design of a neural network based SVC controller, in *Triennial World Congress, IFAC Proceedings*, Prague, Czech Republic, vol. 38, no. 1, 2005, pp. 64–69.
- [10] N. Karpagam and D. Devaraj, Fuzzy Logic Control of Static Var Compensator for Power System Damping, *Int. J. Electr. Comput. Eng.*, vol. 3, no. 4, 2009, pp. 663–669.
- [11] N. Karpagam, D. Devaraj, and P. Subbaraj, Improved fuzzy logic controller for SVC in power system damping using global signals, *Electr. Eng.*, vol. 91, no. 7, 2010, pp. 395–404.
- [12] S. R. Moasheri and M. Alizadeh, Using fuzzy logic power system stabilizer and static VAR compensator to improve power system transient stability, in: *45th International Universities Power Engineering Conf.*, Cardiff, Wales, UK, 31 Aug. - 3 Sept. 2010, pp. 1-5.

- [13] C. Udhayashankar, R. Thottungal, and M. Yuvaraj, Transient stability improvement in transmission system using SVC with fuzzy logic control, in: International Conference on Advances in Electrical Engineering, Vellore, India, Jan. 2014, pp. 1–6.
- [14] P. Singhal and S. Sharma, Hybrid T-I-D and fuzzy logic based SVC controller for transient stability enhancement, *Int. J. Eng. Res. Appl.*, vol. 07, no. 06, 2017, pp. 31–36.
- [15] S. Keskes, N. Bouchiba, S. Sallem, L. Chrifi-Alaoui, and M. Kamoun, Transient stability enhancement and voltage regulation in SMIB power system using SVC with PI controller, in: 6th International Conference on Systems and Control, Batna, Algeria, May 2017, pp. 115–120.
- [16] I. K. Ibraheem, On the frequency domain solution of the speed governor design of non-minimum phase hydro power plant, *Mediterr. J. Meas. Control*, vol. 8, no. 3, 2012, pp. 422–429.
- [17] I. K. Ibraheem, Robust governor design for hydro machines using H_∞ loop-shaping techniques, in: 6th Engineering Conference, University of Baghdad, Baghdad, Iraq, April 2009, pp. 1–10.
- [18] R. A. Maher, I. K. Ibraheem, On the design of robust governors of steam power systems using polynomial and state-space based H_∞ techniques: a comparative study, *Int. J. Electr. Robot. Electron. Commun. Eng.*, vol. 8, no. 8, 2014, pp. 1166–1171.
- [19] I. K. Ibraheem, Design of a two-degree-of-freedom controller for a magnetic levitation system based on lqg technique, *Al-Nahrain Eng. J.*, vol. 16, no. 1, 2013 pp. 1–11.
- [20] I. K. Ibraheem, G. A. Ibraheem, Motion control of an autonomous mobile robot using modified particle swarm optimization based fractional order pid controller, *Eng. Technol. J.*, vol. 34, no. 13, 2016, pp. 2406–2419.
- [21] M. A. Judi, PID based automatic voltage regulator design for a synchronous generator tuned utilizing particle swarm optimization under different damping torque coefficient, *J. Eng. Appl. Sci.*, vol. 13, no. 16, 2018, pp. 6833–6843.

Appendix

System parameter values

$\omega_o = 314$, $D=0.0055$, $H=0.6$, $X_{l1} = 0.45$, $X_{l2} = 0.3$, $Vg=1.1$, $Vt=1$, $B_C = 0.8$, $B_{Lo}= 0.58$, $K =1.2$, $T= 0.2$, $K_c=33.33$.